

# FIRST SIMULATIONS OF TURBULENT TRANSPORT IN THE FIELD-REVERSED CONFIGURATION

C.K. Lau\*, D.P. Fulton\*, J. Bao\*\*, Z. Lin\*\*, T. Tajima\*, L. Schmitz\*\*\*, and the TAE Team\*

\* TAE Technologies  
Foothill Ranch, USA  
Email: clau@tae.com

\*\* University of California, Irvine  
Irvine, USA

\*\*\* University of California, Los Angeles  
Los Angeles, USA

## Abstract

Recent local simulations of the field-reversed configuration (FRC) have reported drift-wave stability in the core and instability in the scrape-off layer (SOL). However, experimental measurements indicate the existence of fluctuations in both FRC core and SOL, although much lower in amplitude in the core. Global nonlinear simulations of the paper resolve this apparent contradiction, showing that fluctuations spread from SOL to core, with the resultant toroidal wavenumber spectra consistent with experimentally measured spectra.

## 1. INTRODUCTION

A field-reversed configuration (FRC) is an elongated prolate compact toroid (CT) with purely poloidal magnetic fields, consisting of two regions separated by a separatrix: an inner, closed field-line core region and an outer, open field-line scrape-off layer (SOL) region. Research interest in the FRC has persisted due to potential reactor benefits: (1)  $\beta$  (the ratio of plasma pressure to magnetic energy density) near unity suggests cheaper magnetic energy costs than low  $\beta$  approaches such as the tokamak; (2) compact shape simplifies construction of the device hull and external magnetic field coils; (3) engineering benefits from the SOL, which naturally occurs and connects to the divertor far from the core; and (4) the lack of toroidal magnetic fields radically changes the magnetic topology and the consequential stability of the plasma.

In recent years at the C-2 FRC experiment, experimental progress by TAE Technologies, Inc. (TAE) led to successful reduction of major macro-instabilities (rotational  $n=2$ , wobble, and tilt  $n=1$  modes[1], where  $n$  is the toroidal mode number). By doing so, they have increased FRC plasma sustainment times to the order of several milliseconds[1,2,3] and pushed this confinement approach into transport-limited regimes[3,4]. Now, an essential step to a viable FRC fusion reactor is to understand the transport processes within FRC plasmas.

Experimental measurements of density fluctuations in the C-2 FRC device[5] have shown that fluctuations of the core and SOL of the FRC exhibit different qualities. In the SOL, the fluctuation spectrum is exponentially decreasing towards electron-scale wavelengths and highest in amplitude towards ion-scale wavelengths. In the core, the fluctuation spectrum is overall lower in amplitude with a dip in the ion-scale wavelengths and a slight peak in electron-scale lengths, which further decrease towards even shorter lengths.

Local linear simulations[6,7,8] using the gyrokinetic toroidal code (GTC)[9] have found qualitatively similar results. The SOL is linearly unstable for a wide range of length scales and varying pressure gradients. In addition, the critical instability thresholds found for the SOL in the local linear simulations are comparable to the experimentally measured fluctuation threshold. On the other hand, the core is robustly stable due to the stabilizing FRC traits of short field-line connection lengths, radially increasing magnetic field strength, and the large finite Larmor radius (FLR)[10] of ions.

While there is also ongoing work towards understanding FRC transport with hybrid kinetic/fluid transport codes, namely Q1D[11] and Q2D[12], the present work is the first global nonlinear gyrokinetic transport study of turbulence in the FRC. We expand on the past linear physics simulations mentioned above to push into the nonlinear kinetic simulations required for understanding turbulence-driven transport.

In this work, global linear simulations also find agreement with previous local linear simulations on core stability and SOL instability. Simulations of a single toroidal mode have demonstrated fluctuations spreading from the SOL region into the core region. Simulations of multiple toroidal modes, confined only to the SOL, show an inverse cascade in the fluctuation spectrum. Finally, global simulations of multiple toroidal modes including both the SOL and core regions find that the combined features of the inverse cascade and turbulence spreading lead to a fluctuation spectrum that is qualitatively comparable to the experimental results of Schmitz *et al.*[5]

## 2. SIMULATION MODEL

In this paper, simulations have been conducted with A New Code (ANC) using gyrokinetic deuterium and adiabatic electrons, without collisions, in a C-2-like magnetic geometry. ANC is a global, gyrokinetic, particle-in-cell (PIC) simulation code[13,14,15], suitable for simulation of electrostatic drift-wave turbulence. In this work, electrostatic perturbative  $\delta f$  simulations[16,17,18,19,20] are confined to a nonlocal domain spanning the confinement vessel region of the reactor with periodic boundaries in the axial directions and neglecting parallel outflow effects. As shown in Fig. 1, the magnetic field null region is excluded in these simulations to preserve gyrokinetic validity. These are initialized with an FRC equilibrium[21] with density and ion temperature gradients and flat electron temperature corresponding to Table 1.

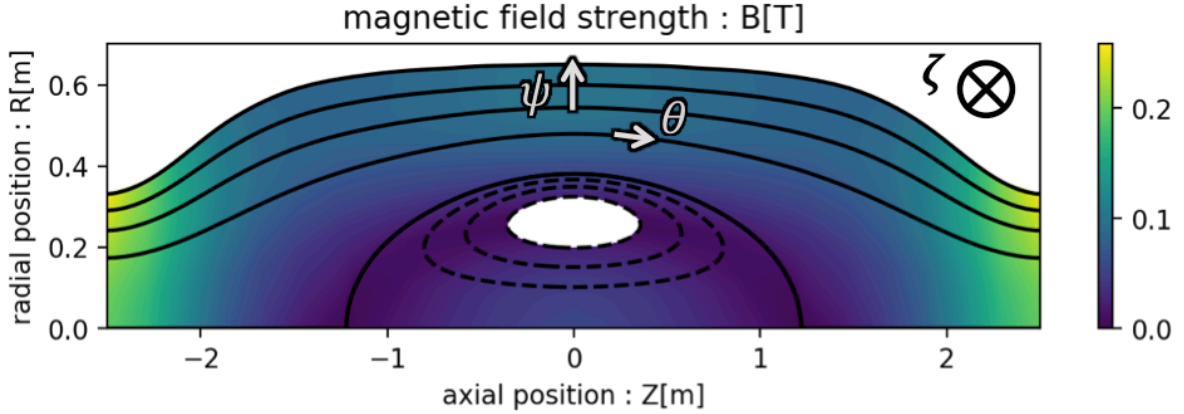


Fig. 1 – The equilibrium FRC magnetic field is shown. Note that the magnetic field null region ( $Z=0\text{m}$ ,  $R\sim 0.25\text{m}$ ) is not included in the simulation domain. The black lines correspond to drift-surfaces corresponding to different poloidal flux contours. The magnetic coordinate system referred to within the paper is also shown:  $\hat{\psi}$  is the direction of radially increasing poloidal flux,  $\hat{\theta}$  is the direction along the magnetic field-lines, i.e. poloidal, and  $\hat{\zeta}$  is the direction about the machine axis, i.e. azimuthal or toroidal.

TABLE 1. Simulation parameters in units of cm at  $R=53\text{cm}$ , the distance from the machine axis.

$L_{T,i}$	$L_{T,e}$	$L_n$	$\rho_i$	$\rho_e$
5.36	$\infty$	5.36	1.1	0.022

In Sec. 3, the simulation domain extends from the SOL to the core but only allows for a single toroidal mode ( $n=20$  is shown). In Sec. 4, the simulation domain is confined to the SOL but allows for multiple toroidal modes ( $n=\{5,10,\dots,75,80\}$ ). In Sec. 5, the simulation domain extends from the SOL to the core and allows for multiple toroidal modes ( $n=\{0, 5,10,\dots,75\}$ ). The factors of 5 in the toroidal modes selected in Sec. 4 and 5 are due to the numerical reduction of the toroidal domain into a wedge of the full toroidal domain. Simulations of a smaller toroidal wedge (factors of 10) yield similar results in saturation levels and toroidal spectra.

## 3. FLUCTUATIONS SPREADING FROM SCRAPE-OFF LAYER TO CORE

With the equilibrium and model as described in Sec. 2, linear simulations of a single toroidal mode show exponential growth of instability in the SOL with toroidal propagation in the ion diamagnetic direction.

Comparison with local linear theory indicates that this is a slab-like ion temperature gradient (ITG) drift-wave instability[15].

In previous local, linear simulations [8], the SOL was found to be unstable while the core was stable. A variety of effects were studied, and core stability was found to be due to the stabilizing FRC traits of (1) short electron transit length, (2) radially increasing magnetic field, and (3) strong FLR effects due to weak magnetic field. In the initial linear simulations of this section, nonlocal effects were numerically removed, effectively localizing the physics of the simulations. Consistent with past local simulations, there is no mode growth in the core due to the stabilizing effects mentioned, although the short electron transit effect is enhanced by only including the electron adiabatic response in our equations.

In contrast to the past work, realistic nonlocal physics can be included through the Laplacian in the Poisson equation and through the gyroaveraging in the particle model. With these nonlocal effects included, drift-surfaces of different poloidal flux labels  $\psi$  are physically coupled. This introduces a radial wavenumber  $k_{\psi}$  into the wave dispersion, allowing for radial wave propagation such that a radial eigenmode structure forms across the SOL and core. Despite the physical coupling, in linear simulations, the amplitude of the formed structure in the core is lower than in the SOL by more than a factor of 100. When nonlinear  $\delta\vec{E}\times\vec{B}$  effects are included in the simulations, the instability saturates and the fluctuation amplitude in the core rises to a magnitude lower than the SOL by about a factor of 10.

This process can be seen in the bottom panel of Fig. 2 which shows the mode amplitude in the core and SOL: initially, the unstable mode first grows in the SOL but has not started to grow in the core; at  $t \approx 0.5\text{ms}$ , the radial eigenmode has formed such that the mode amplitude in the core is growing at the same growth-rate. This whole process is also shown in the top panel of Fig. 2, which shows the mode growing in the SOL first before spreading into the core.

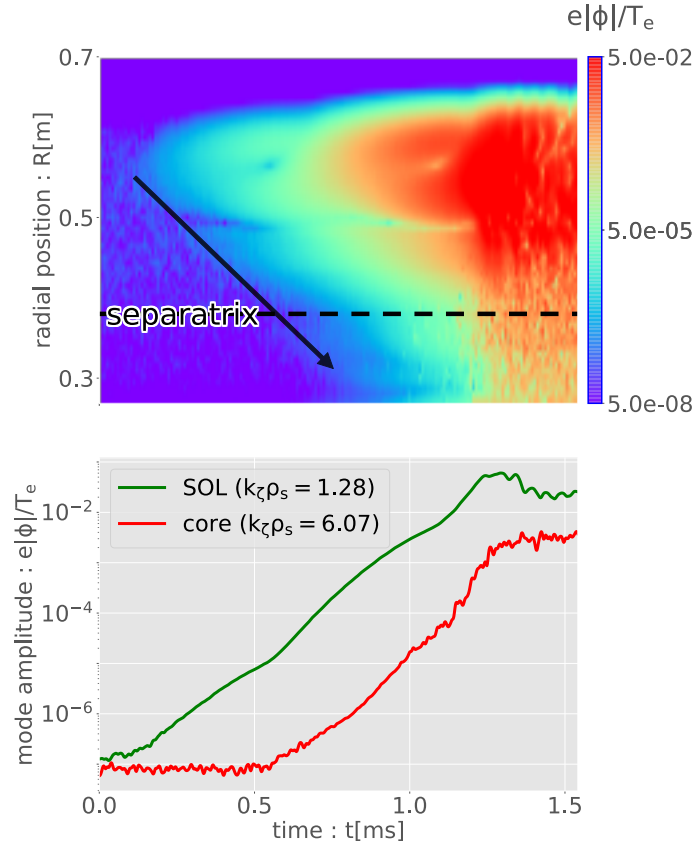


Fig. 2 – (TOP) The magnitude of the electrostatic potential along the outer midplane,  $\phi(R, Z = 0, t)$ , is shown with the colorbar following a logarithmic scale, and the dashed line indicates the location of the separatrix. (BOTTOM) Line-outs from the top plot corresponding to the SOL and core regions are shown in green and red, respectively.

When particles are allowed to experience nonlinear  $\delta\vec{E}\times\vec{B}$  effects in the simulations, the mode saturates at a SOL mode amplitude of about  $e\phi/T_e \sim 5\times 10^{-2}$  as seen in Fig. 2 at  $t \approx 1.25$ ms. On the other hand, the saturation level in the core is about a factor of 10 lower than in the SOL, consistent with experimental measurements showing lower fluctuation amplitudes in the C-2 core[5].

#### 4. INVERSE SPECTRAL CASCADE IN THE SCRAPE-OFF LAYER

In the simulations of this section, the simulation domain is limited to the SOL to focus on the characteristics of SOL turbulence. Because turbulence requires intermixing of multiple toroidal modes, simulations of this section allow for the inclusion of multiple toroidal modes ( $n=\{5,10,\dots,75,80\}$ ) where the toroidal modes  $n=\{5,10,15\}$  were previously found to be linearly stable or damped modes.

The modes saturate at  $e\phi/T_e \sim O(10^{-2})$  as seen in the top panel of Fig. 3. Since the saturation levels of the multiple-mode simulations are comparable to the single-mode simulations, the main saturation mechanism is unchanged despite the change in simulation domain, and the physics of these multiple-mode simulations confined to just the SOL region remain valid and valuable for FRC simulations which include the core region.

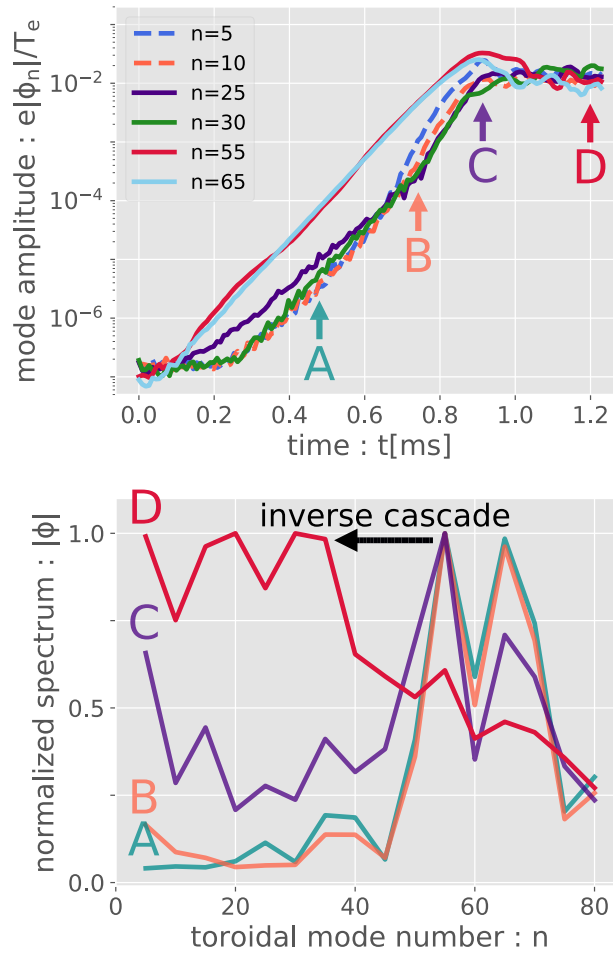


Fig. 3 – (TOP) The magnitude of the electrostatic potential is shown for several toroidal modes (only a subset of the modes in the simulation are shown for clarity). (BOTTOM) The toroidal modenumbers spectra corresponding to times marked in the top plot are shown. Here, the spectra are normalized by the maximum value for qualitative comparison for different times.

Initially, the largest and fastest growing modes of this simulation are  $n = 55$  and  $n = 65$ . In these simulations, different modes can couple to each other through the beating of two waves exciting a third, when wave matching conditions ( $\vec{k}_1 + \vec{k}_2 = \vec{k}_3, \vec{\omega}_1 + \vec{\omega}_2 = \vec{\omega}_3$ ) are met. Because lower toroidal mode numbers can more easily satisfy these matching conditions, an inverse toroidal spectral cascade occurs from the higher amplitude shorter wavelength modes to the linearly stable longer wavelength modes.

This process can be seen dynamically in the top panel of Fig. 3 which shows a subset of the simulated modes: at (A), the highest amplitudes belong to the high- $n$  modes; at (B), the linearly stable low- $n$  modes (dashed lines) have overtaken some of mid- $n$  modes and the nonlinear coupling is suggested by the growth-rates which are roughly twice the value of the linearly unstable modes; at (C), the modes are saturating but the inverse cascade continues and the high- $n$  modes are beginning to lower in amplitude; and at (D), some time after saturation, the high- $n$  modes are the lowest in amplitude while the low- $n$  modes are the highest. Snapshots of the spectrum corresponding to these four times are also shown in the bottom panel of Fig. 3. Overall, this cascade corresponds to a change from an average wavelength of  $\langle k_\zeta \rho_s \rangle \sim 3$  during the linearly growing phase, (A) and (B), to an average wavelength of  $\langle k_\zeta \rho_s \rangle \sim 1.9$  after the nonlinear cascade, (D).

## 5. GLOBAL TURBULENCE FROM SCRAPE-OFF LAYER TO CORE

In this section, the simulations of multiple toroidal modes ( $n = \{0, 10, \dots, 70\}$ ) now span both the SOL and core regions. As in Sec. 3, with the inclusion of the core region, instability grows in the SOL, but fluctuations can now spread into the core. In addition, with multiple toroidal modes as in Sec. 4, energy cascades from the unstable shorter wavelength modes to the longer wavelength modes. Together, these two processes shape the toroidal spectra of the FRC core and SOL as shown in Fig. 4.

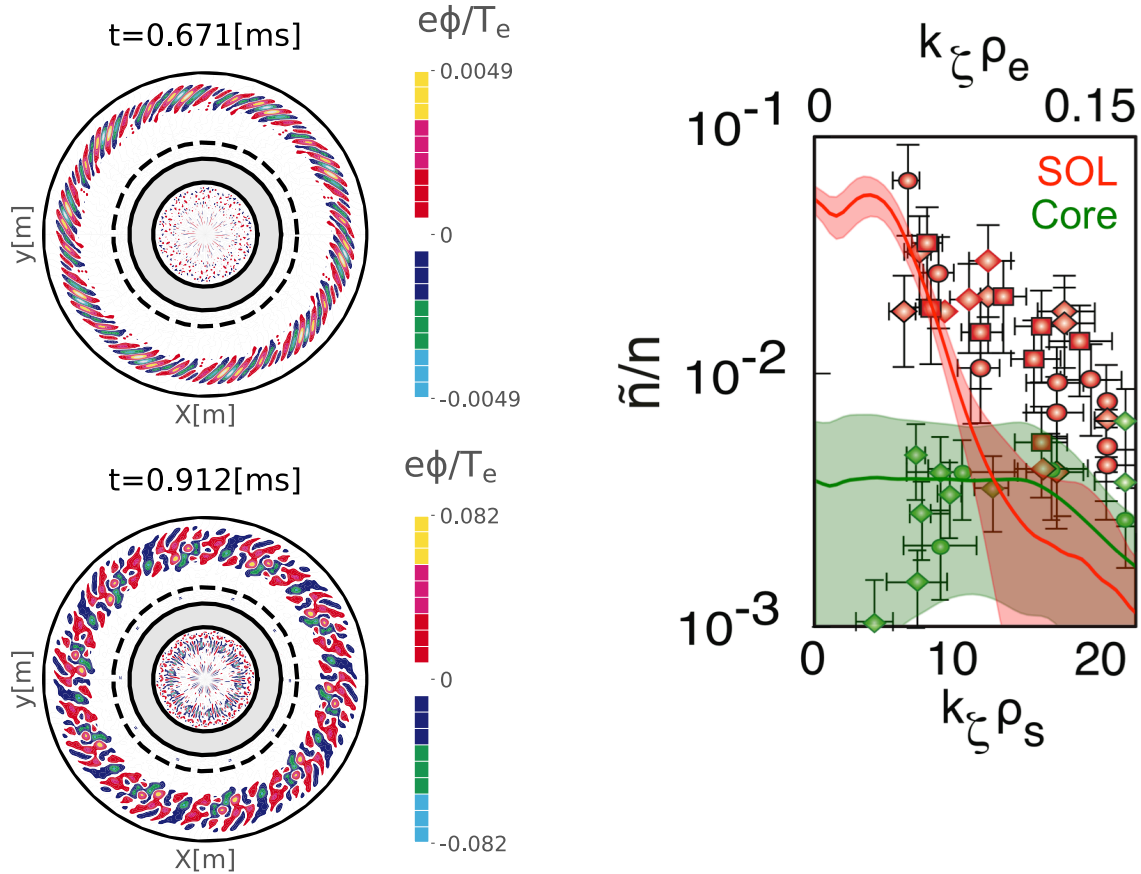


Fig. 2 – (LEFT) The electrostatic fluctuation is shown at the exponential growing stage (TOP) and after saturation (BOTTOM) as viewed along the machine axis at  $Z=0$ . (RIGHT) The fluctuation spectrum corresponding to the post-saturation time from simulation is plotted as the lines while the spectrum corresponding to the experimental measurements is plotted as data points. The shaded region indicates the standard deviation of the simulation spectrum over the time period for which this data represents. The deviation over the time period is smaller for longer wavelengths in the SOL where the instability exists.

The electrostatic potential mode structures, viewed along the machine axis at the center of the confinement vessel, from times corresponding to linear growth ( $t = 0.671$ ms) and nonlinear saturation ( $t = 0.912$ ms) are shown in the left side of Fig. 4. The dashed line corresponds to the separatrix, and the grey region is the region near the null point, which is not included within the simulation domain due to gyrokinetic validity. (Note that

the inner core region is connected to the outer core region through the parallel direction itself, as seen in the equilibrium magnetic field in Fig. 1.)

Consistent with the simulations of Sec. 3 and Sec. 4, fluctuations are lower in amplitude in the core and an inverse cascade is observed. The inverse cascade can be graphically seen from the change in the short wavelength mode structures in the top left panel to the larger scale turbulent eddies in the bottom panel. Due to turbulence spreading, the fluctuations in the core also become more comparable in magnitude and more visible after saturation in the bottom left panel of Fig. 4.

In the right panel of Fig. 4, the toroidal wavenumber spectrum from simulation is calculated from integrating the electrostatic potential along the outer midplane at  $Z=0$  and binned according to toroidal wavenumbers (where  $k_z = n/R$ ) for a duration between  $t = 0.949 \sim 1.03$ ms. The mean simulation spectrum is plotted as the solid lines with green (red) corresponding to the spectrum calculated from the core (SOL) region. The deviation over time for the spectra is plotted as the corresponding shaded regions in the figure. In comparison, the experimental measurements of density fluctuations[5] is plotted as the scatter points.

The shape of this fluctuation spectrum is qualitatively consistent with the experimentally measured density fluctuation spectrum[5]. Fluctuations in the SOL are largest at long wavelengths and decrease towards shorter wavelengths due to the inverse cascade. Fluctuations in the core are much lower than in the SOL due to the origin of the fluctuations being from outside of the core. Although core fluctuations may appear to be higher in amplitude at longer wavelengths in the simulation than shown by experiments, this is because the fluctuations in the core originate from the SOL and so the amplitude varies over time. As shown by the shaded regions in the plot, the deviation over time covers a range that would fall within the experimental measurements.

## 6. CONCLUSION

In this paper, the simulation model has been extended to include nonlinear particle effects and interaction of multiple toroidal modes in a global geometry which includes both the core and SOL regions in the FRC confinement vessel. Previous local linear simulations found linear modes to be stable in the FRC core but unstable in the SOL[6,7,8]. Consistent with these past simulations, linear simulations in the current work also finds instability in only the SOL region. These results are in qualitative agreement with experimental measurements of density fluctuations in the C-2 FRC plasmas, which show core fluctuations to be lower in amplitude than SOL fluctuations[5].

As shown in Fig. 4, with the updated global model, the current work can now go beyond qualitative comparison and directly compare with experimental measurements. Nonlinear simulations show that instability saturates at levels comparable to experimentally measured amplitudes. An inverse spectral cascade produces a SOL toroidal wavenumber spectrum that decreases towards shorter wavelengths. In addition, the fluctuations spread from the SOL into the core at reduced amplitudes and shorter wavelengths, which produces a core toroidal wavenumber spectrum that is much lower in amplitude at longer wavelengths. These simulated wavenumber spectra agree with the experimentally measured spectra in several features: (1) lower amplitude in the core at longer wavelengths, (2) higher amplitude in the SOL at longer wavelengths, (3) decreasing trend towards shorter wavelengths in the SOL.

The wavenumber spectrum found in experiments and simulations is favourable for confinement in the FRC core: lower amplitude long wavelength fluctuations lead to lower levels of transport. The work of the paper has shown that this spectrum arises from SOL fluctuation spreading and not from inherent core instabilities. Because the core is stable to electrostatic drift-instabilities[8] due to the effects of typical FRC features (magnetic well, short electron field-line transit along, and large FLR), core turbulence in future devices or different equilibria is also likely to originate from outside instabilities, and the fluctuation spectrum is expected to remain favourable for confinement.

Although the current work has extended previous simulation models, there are important physics present in experiment which have not been included. In previous local linear simulations, a drift-kinetic electron model was used and allowed for a trapped electron mode to arise in the SOL. Because this global FRC simulation is the first of its kind, we started with a simpler model using an adiabatic electron response. This may explain the discrepancy in the simulated SOL wavenumber spectrum, which shows slightly longer wavelengths than experiments. In upcoming work, the electron model will be extended to drift-kinetic electrons to allow for such a trapped electron mode to arise. In addition equilibrium sheared flows are experimentally present but have not

been included in this work. These sheared flows can modify the properties of linear instabilities and nonlinear turbulent structures. Future work will also include and quantify the effects of equilibrium sheared flows.

## ACKNOWLEDGEMENTS

The authors would like to thank S. Dettrick and the TAE team at TAE Technologies, Inc., for equilibrium data as well as ongoing insights and collaboration in the development of these simulations. Portions of this work were carried out at University of California, Irvine with the support of the Norman Rostoker Fellowship (Grant No. TAE-200441). Simulations used the resources of DOE Office of Science User Facilities: National Energy Research Scientific Computing Center (DOE Contract No. DE-AC02-05CH11231) and Innovative and Novel Computational Impact on Theory and Experiment (INCITE) program at Argonne Leadership Computing Facility at Argonne National Laboratory (DOE Contract No. DE-AC02-06CH11357).

## REFERENCES

- [1] GUO, H.Y., BINDERBAUER, M.W., TAJIMA, T., MILROY, R.D., STEINHAEUER, L.C., YANG, X., GARATE, E.G., GOTA, H., KOREPANOV, S., NECAS, A., ET AL., Achieving a long-lived high-beta plasma state by energetic beam injection, *Nat. Comm.* **6** (2015).
- [2] TUSZEWSKI, M., SMIRNOV, A., THOMPSON, M.C., AKHMETOV, T., IVANOV, A., VOSKOBOYNIKOV, R., BARNES, D.C., BINDERBAUER, M.W., BROWN, R., BUI, D.Q., ET AL., A new high performance field reversed configuration operating regime in the C-2 device, *Phys. Plasmas* **19** 056108 (2012).
- [3] BINDERBAUER, M.W., TAJIMA, T., STEINHAEUER, L.C., GARATE, E., TUSZEWSKI, M., SCHMITZ, L., GUO, H.Y., SMIRNOV, A., GOTA, H., BARNES, D., ET AL., A high performance field-reversed configuration, *Phys. Plasmas* **22** 056110 (2015).
- [4] BINDERBAUER, M.W., ET AL., “Recent breakthroughs on C-2U: Norman’s legacy”, the Physics of Plasma-Driven Accelerators and Accelerator-Driven Fusion: The Proceedings of Norman Rostoker Memorial Symposium, AIP Publishing, Melville, NY (2016).
- [5] SCHMITZ, L., FULTON, D.P., RUSKOV, E., LAU, C., DENG, B.H., TAJIMA, T., BINDERBAUER, M.W., HOLOD, I., LIN, Z., GOTA, H. ET AL., Suppressed ion-scale turbulence in a hot high- $\beta$  plasma, *Nat. Comm.*, **7** (2016).
- [6] FULTON, D.P., LAU, C.K., HOLOD, I., LIN, Z., AND DETTRICK, S., Gyrokinetic particle simulation of a field reversed configuration, *Phys. Plasmas* **23** 012509 (2016).
- [7] FULTON, D.P., LAU, C.K., SCHMITZ, L., HOLOD, I., LIN, Z., TAJIMA, T., BINDERBAUER, M.W., AND THE TAE TEAM, Gyrokinetic simulation of driftwave instability in field-reversed configuration, *Phys. Plasmas* **23** 056111 (2016).
- [8] LAU, C.K., FULTON, D.P., HOLOD, I., LIN, Z., BINDERBAUER, M., TAJIMA, T., AND SCHMITZ, L., Drift-wave stability in the field-reversed configuration, *Phys. Plasmas* **24** 082512 (2017).
- [9] LIN, Z., HAHM, T.S., LEE, W.W. TANG, W.M., AND WHITE, R.B., Turbulent transport reduction by zonal flows: Massive parallel simulations, *Science* **281** (5384) (1998).
- [10] ROSENBLUTH, M., KRALL, N., AND ROSTOKER, N., Finite Larmor radius stabilization of “weakly” unstable confined plasmas, *Nucl. Fusion Supp.* **1** 143 (1962).
- [11] GUPTA, S., BARNES, D.C., DETTRICK, S.A., TRASK, E., TUSZEWSKI, M., DENG, B.H., GOTA, H., GUPTA, D., HUBBARD, K., KOREPANOV, S., ET AL., Transport studies in high-performance field-reversed configuration plasmas, *Phys. Plasmas* **23** 052307 (2016).
- [12] ONOFRI, M., YUSHMANOV, P., DETTRICK, S., BARNES, D., HUBBARD, K., AND TAJIMA, T., Magnetohydrodynamic transport characterization of a field reversed configuration, *Phys. Plasmas* **24** 092518 (2017).
- [13] FULTON, D.P. Kinetic simulation of edge instability in fusion plasmas, doctoral dissertation, University of California, Irvine, 2015.
- [14] FULTON, D.P., LAU, C.K., HOLOD, I., LIN, Z. AND DETTRICK, S., A New Code (ANC): global, cross-separatrix, turbulent transport particle-in-cell code, manuscript-in-preparation, TAE Technologies, Foothill Ranch, CA, 2017.
- [15] LAU, C.K., Electrostatic turbulence and transport in the field-reversed configuration, doctoral dissertation, University of California, Irvine, 2017.

- [16] TAJIMA, T., "Guiding-center method", Computational Plasma Physics: With Applications to Fusion and Astrophysics, Addison-Wesley, Redwood City, CA (1989).
- [17] DIMITS, A.M. AND LEE, W.W., Partially linearized algorithms in gyrokinetic particle simulation, J. Comput. Phys. **107** 2 (1993) 309–323.
- [18] PARKER, S.E. AND LEE, W.W., A fully nonlinear characteristic method for gyrokinetic simulation, Phys. Fluids B: Plasma Phys. **5** 1 (1993) 77–86.
- [19] LIN, Z., NISHIMURA, Y., XIAO, Y., HOLOD, I., ZHANG, W.L. AND CHEN, L., Global gyrokinetic particle simulations with kinetic electrons, Plasma Phys. and Control. Fusion **49** 163 (2007).
- [20] HOLOD, I., ZHANG, W.L., XIAO, Y. AND LIN, Z., Electromagnetic formulation of global gyrokinetic particle simulation in toroidal geometry, Phys. Plasmas **16** 122307 (2009).
- [21] GALEOTTI, L., BARNES, D.C., CECCHERINI, F., AND PEGORARO, F., Plasma equilibria with multiple ion species: equations and algorithm, Phys. Plasmas **18** 082509 (2011).